



# ENHANCING A NOVEL NEURAL NETWORK ALGORITHM FOR FORECASTING THE IDENTIFICATION OF SHAPES AND DEFECTS IN POLYMER CONCRETE PANELS

Vinod Mansiram Kapse<sup>1</sup>  
Arun Kumar Marandi  
Beemkumar Nagappan  
Ankita Agarwal

Received 12.11.2023.  
Received in revised form 16.01.2024.  
Accepted 26.01.2024.  
UDC – 004.032.26

Keywords:

*Polymer concrete (PC), Stochastic  
Raven Roosting Optimization  
Enhanced Artificial Neural Network  
(SRRO-EANN), Concrete, Panel*

A B S T R A C T

*The increased durability and performance features of polymer concrete panels have led to their widespread application in construction. The manufacturing of precise and effective techniques for identifying forms and flaws is vital to guarantee the high quality of these panels. To increase the accuracy of structure and defect-recognition in polymer concrete panels, this study presents a new Stochastic raven roosting optimization enhanced artificial neural network (SRRO-EANN) forecasting technique. The data sample used to assess the completed model fits the training dataset is referred to the test dataset. The Gaussian filter (GF) is a tool used in the pre-processing and Principal Component Analysis (PCA) feature extraction, leading to more effective utilization and understanding the defect capturing. The findings of the research indicate the effectiveness for the future development of forecasting technologies in the realm of quality control and building material inspection.*



© 2024 Published by Faculty of Engineering

## 1. INTRODUCTION

Polymer concrete (PC) is a type of construction particle composite also known as cement-like a combination, in which a polymer binder has completely taken the location of cement paste. It is made by combining pre-polymers, monomers, or synthesized resins with an appropriate aggregate that allowing the resin binder to solidify. The interaction between the resin and the hardener causes the PC binders, which are typically two-component sets, to set and harden. PC may include a binder that has been

hardened by polymerization without byproducts such as polyester or epoxy resin by polymerization, together with the release of a byproduct (Nagajothi and Elavenil (2020)). With high compressive strength and excellent chemical resistance, PCs have several unique benefits, including exceptional adherence to a wide range of substrates as well as prompt responsiveness to exploitation. Selecting the suitable material composition to create composites with predictable qualities is essential to the utility and longevity of PC composites. However, detrimental atmospheric, chemical, and biological elements are exposed to living PC

<sup>1</sup> Corresponding author: Vinod Mansiram Kapse  
Email: [director@niet.co.in](mailto:director@niet.co.in)

composites throughout usage, which might result in the material's slow deterioration and destruction (Dhiman et al., (2020)). It examines the significance nanoparticles are in preventing the erosion and degradation of building materials. The article explores processes and methods for improving the reliability of building materials by investigating its use at the nanoscale.

Consequently, a crucial concern is the systematic evaluation of PC component durability and diagnostics. Non-destructive testing (NDT) allows information on the properties of a material to be collected without damaging its microstructure and serviceability, in contrast to destructive techniques. In addition, the most popular non-destructive procedures in substance science and industry are ultrasonic techniques (Dolati et al., (2023)). They are well-known and regulated to be utilized with conventional construction materials, such as rocks, cement, and metals. Impact damage is a common and intricate characteristic that consists of overlapping delamination of various sizes and shapes and randomly dispersed middle and lateral fractures. On a composite construction, transverse impacts account for the majority of the effects (Asteris et al., (2021)). Impact damage has been categorized by several academics, although there isn't a distinct division between them. Depending on the speed of impact, impact damage is classified as low-velocity impact (LVI), high-velocity impact, and hyper-velocity impact. The highest limit of human hearing frequency, 20 kHz is exceeded by longitudinal elastic waves, or vibrations, which are used in the UPV technique. Higher frequency vibrations are utilized to get precise measurements. However, ultrasonic pulses have lesser energy due to increased attenuation (Fodil et al., (2021)). Consequently, the highest frequency sound waves that enable the recording of high-quality waveforms following signal passage through a medium should be used for the ultrasonic testing of heterogeneous concrete composites. Medium particles vibrate in a direction parallel to the wave's path due to longitudinal waves. Solids, liquids, and gases may be traversed by this particular type of motion. Due to its excellent durability and adaptability over traditional concrete, polymer concrete has become a crucial component of contemporary buildings by (Yang and Zhang (2023)). Blending aggregates with thermosetting resin, its composition makes it an excellent option for a wide range of applications, from architectural advances to

Guaranteeing the structural soundness of polymer concrete panels necessitates a strategy to recognize and tackle any forms and flaws that can emerge during production or operation. Sophisticated forecasting methods that may be used in the production of polymer concrete panels have been made possible by machine learning and artificial intelligence developments. Modern forecasting techniques, including computer vision, neural networks, and predictive analytics, are briefly reviewed in this section, along with how they are used explicitly in form recognition and panel

defect detection (Li et al., (2020)). In order to improve quality control procedures in the manufacturing of polymer concrete panels, this study investigate and clarify the role that forecasting approaches play in addressing these issues.

## 1.1 Key contributions

- The requirement for accurate identification techniques to guarantee the panels' excellent quality is highlighted by their increased longevity and higher performance characteristics.
- In order to gather the pressing need to improve polymer concrete panel form and defect identification accuracy, this study introduces a new forecasting method called the SRRO-EANN.
- The findings of this study show bright futures for forecasting technology in the field of building material quality management and inspection.
- The performance metrics provided highlight the usefulness and efficiency of the suggested method, which makes a significant contribution to the continuous efforts to improve the performance and dependability of polymer concrete materials in building applications.

For context and understanding, we include a comprehensive literature review in section 2. Section 3 offers an in-depth analysis of the methodology. We provide a result and discussion in section 4. We provide a conclusion in Section 5.

## 2. RELATED WORKS

Mansourdehghan et al., (2022) presented a system for assessing damage to reinforced concrete shear walls based on visual characteristics such as aspect ratio, crushing area density, distribution of crack patterns, and boundary condition existence. Evaluating the damaged walls' level of performance and estimating the walls' continuing strength as well as drifting proportion are the two main components of the study. Rautela et al., (2022)) offered two distinct unsupervised-feature training techniques in which the neural networks are educated on foundation situations to acquire knowledge of the fundamental signal distributions. The need for strong and dependable monitoring of structural health protocols for aerospace composite frameworks was rising quickly due to the adoption of impairment tolerance-based engineering principles. Amin et al., (2022) looked at the nonlinear potential of gene expression programming modeling based on artificial intelligence to create a surface bonding capacity of fiber-reinforced polymeric layers mounted on a reinforced concrete prismatic with slits could be calculated mathematically. Steel reinforcement corrosion requires regular maintenance and repairs

for reinforced concrete structures. Refitting beams, slabs, columns, and joints is an everyday use for fiber-reinforced polymer (FRP) laminates. Badra et al., (2022) investigated the punching shear strength of FRP-reinforced concrete slabs, a complicated behavior influenced by several factors and multiple processes. More precise and consistent strength models are required, as demonstrated by this study's evaluation of a chosen strength models from the literature utilizing a streamlined reliability analysis approach. Cakiroglu et al., (2022) provided an alternative method to forecast the axial capacity of fiber-reinforced polymer- reinforced concrete (FRP-RC) columns by leveraging the power of artificial intelligence. Because of their improved mechanical qualities and exceptional ability to withstand corrosion, FRP rebar was utilized in RC components in place of steel rebar. Rezaiee-Pajand et al., (2021) looked at how flexing crack distribution was affected by the lap-sliced size, cycle quantity, fiber steel %, longitudinally reinforcement width, the compression strength of building materials, the cross-section elevation and breadth. Reducing the gaps between flexural fractures is one of the most important ways to prevent corrosion on reinforcements. Dunaj et al., (2020) focused on problems associated with modeling steel-polymer concrete frames for machine tools. The physicality of the modeled phenomena was investigated as the foundation for the activities that were done and the models that were suggested. The creation of a compelling technique for modeling steel-polymer concrete buildings using the posteriori methodology is one of the most significant accomplishments. Cheng and Shen (2021) introduced an infrared thermograph-based semi-real-time detection technique. In order to locate the subsurface voids based on the regional temperature differential, the devised approach makes use of the hydration heat throughout the curing phase. When building concrete pavements, subsurface consolidation faults are a frequent problem. These concealed flaws frequently need expensive repairs after the project is completed. Rezakhani et al., (2021) determined, by numerous laboratory tests and numerical modeling, how different kinds of steel fibers affected the quasi-static mechanical behavior of ultra-high performance concrete (UHPC). While fiber size and shape significantly affected flexural and tensile characteristics, they had no effect on the quasi-static properties of UHPC under compression. Liu et al., (2020) investigated the effects of re-dispersible polymeric emulsified particles on the dynamic compression properties of CFRPC (carbon fiber-reinforced polymer concrete) by testing methods. To evaluate the effect of emulsion powdered on CFRPC, the durability, distortions, and dynamic compression strength of the tested samples have been investigated.

### 3. MARTIAL AND METHODS

The assessment dataset is a sample of data that is used to evaluate or not the model matches with the training data and then pre-processed using the Gaussian filter (GF) and feature extraction for Principal component analysis (PCA). The suggested block diagram is shown in Figure 1.

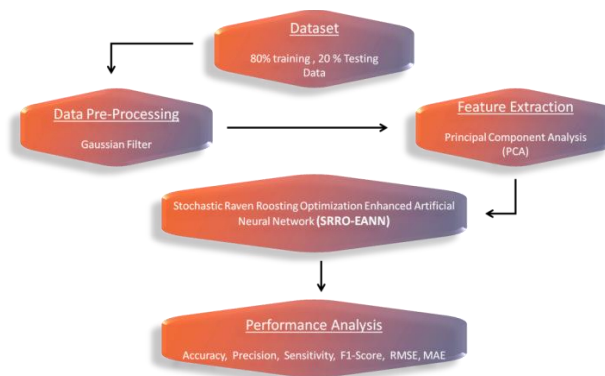


Figure 1. Block diagram of the proposed model

#### 3.1 Dataset

The database aggregates images from many data repositories, SDNET 2018, including Chundata, and data taken from residential structures. Negative (non-cracked) and Positive (cracked) images sets were created from the dataset. They were kept in separate folders with 11,000 and 11,000 RGB-formatted images in each, marked as cracked and non-cracked. A total of 4400 images were not utilized for training, but for testing. 80% of Training and 20% of testing data collection were divided apart. The model's assessment began to rise immediately as the layout integrated the validation data collection skill. The assessment dataset is a portion of the data used to assess the model aligns with the training data collection (Philip et al., (2023)). A subset of the data called the assessment data collection is used to evaluate the model's degree of alignment with the training dataset in an unbiased manner.

#### 3.2 Data pre-processing using Gaussian filter (GF)

Gaussian filtering known as Gaussian blur, is a method for lowering noise in images. A function known as the Gaussian is used in Gaussian filtering, a type of image-blurring filter, to calculate the change that is applied to each pixel in the image. Convolution is a necessary step in the Gaussian filtering process. Convolution is the outcome of multiplying the whole matrix by the point (y, w) in the image's surrounding extension.

$$H_0(w, z) = Bf \frac{-\frac{(w-\mu_w)^2}{2\sigma_w^2}}{2\sigma_w^2} + \frac{-\frac{(z-\mu_z)^2}{2\sigma_z^2}}{2\sigma_z^2} \quad (1)$$

$\mu$ -mean,  $\sigma$ -varian (y and x variable).

### 3.3 Principal component analysis (PCA) for feature extraction

In order to reduce the size of the new index, many significant elements may be transformed using PCA into no important index if a function eliminates extraneous data and offers a index linked to the chance of occurrences. The PCA stages are as follows: In order to obtain the index  $F$  sample matrix and establish the index elements, the research-worthy field is chosen.

$$F = (F_{ij})C * B \quad (2)$$

$$\text{Where } j = 1,2, \dots, A, j = 1.2 \dots, B \quad (3)$$

matrix with eigenvalues within the necessary range of  $1 \geq b \geq 0$ . The procedure for the PCA expression as follows:

$$T_i = F_{ej} \quad (4)$$

The contested athletic event  $Y$  has the following particular risk rating,

$$x = aY_1 + cY_2 + \dots + bY_x \quad (5)$$

Where  $Y$  is an Eigen value of the eigenvector  $b$  and  $x$  is the normalized value's start date.

### 3.4 Stochastic raven roosting optimization enhanced artificial neural network (SRRO-EANN)

A novel method for predicting and spotting forms and flaws in polymer concrete panels is called SRRO-EANN. To overcome obstacles in the field, this technique blends the capability of artificial neural networks with stochastic optimization. The stochastic optimization part adds randomization to the search procedure by taking inspiration from raven roosting behavior. SRRO-EANN is enhanced to explore the solution space and find a variety of neural network parameter settings. This is useful for defect and form recognition, where the landscape of possible solutions might be complex and diverse.

#### 3.4.1 Enhanced Artificial Neural Network (EANN)

The neural networks of a biological nerve network are replicated by computational systems called Enhanced Artificial Neural Networks (EANN). Given that the basic building blocks of EANNs are based on the anatomy of the brain, even the terminology employed is borrowed from the field of neuroscience. The primary grouping of the rudimentary artificial neurons is called an EANN. By building layers and connecting them, this clustering is achieved. This procedure may be used in many optimization techniques. A multi-layer feed-forward EANN setup is shown in the top portion of Figure 2. EANNs are

generally constructed using three layers: input, output, and hidden layers. For practical purposes, hidden layers may consist of a single layer or many layers. There are varying numbers of neuronal components in each layer. The connections between these components dictate how the network functions, much like in evolution. The relationship between the input vector  $W_j^{(m)}$  as well as the resulting matrix  $W_i^{(m+1)}$  the following may be said about this element:

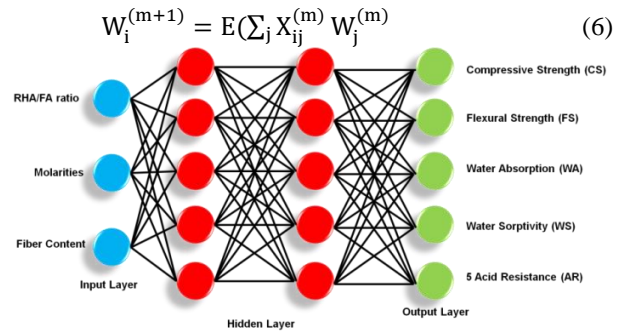


Figure 2. Architecture of EANN

$E(w)$ , the function that is tan-sigmoid  $E(w) = \frac{1}{1 + e^{-w}}$  or another transfer function that is nonlinear, Log-sigmoid function, for example, and  $W_i^{(m+1)}$  is the unit's output,  $i$  in the  $m$ th layer  $X_{ij}^{(m)}$  is a mass in units  $j$  in  $m$ th layer to unit  $j$  in  $(m + 1)$ th layer. The input layer's units are shown as input vector. The next layer's units add up the weighted sum of the input and output the outcome of applying a nonlinear function to the total. Using the least sum squared optimality criteria of errors between the anticipated and desired values, the learning process is based on an exponential pursuit:

$$F = \sum_{o=1}^o (c_o - p_o)^2 \quad (7)$$

The sum squared error overall  $F$  is calculated by averaging every pattern in the training set,  $c_p$  is the intended result (estimated) for the  $o$ th design, and  $p_o$  is the output as it is actually measured. All of the connected nodes' weights are changed during the reduction process until the maximum number of cycles or the intended error level is attained. The learning algorithm used for the weights is :

$$X_{ij}^{(m)}(s + 1) = X_{ij}^{(m)}(s) + \Delta X_{ij}^{(m)}(s) \quad (8)$$

$$\Delta X_{ij}^{(m)}(s + 1) = -\eta \frac{\partial F}{\partial F_{ij}^{(m)}} + \mu \Delta X_{ij}^{(m)}(s) \quad (9)$$

$X_{ij}^{(m)}(s)$  is the signal for teaching the correct response at the  $s$ th learning step.  $\Delta X_{ij}^{(m)}(s)$  is the weight correction at the  $\eta$  is the learning rate,  $s$ th learning step, and  $\mu$  is the momentum factor,  $\eta$  is an

incremental setting that modifies the correction each time, and  $\mu$  decreases oscillation and promotes quick convergence. Network learning is aided by these parameters having the right values. A proportional transmission function is used between the hidden and output layers to prevent the outcome from being restricted to a narrow range. Assuming there are indeed enough neurons in the sigmoid layer of the two-layer sigmoid and linear network, it is expected to be able to represent any functional interaction between input and output.

### 3.4.2 Stochastic raven roosting optimization (SRRO)

SRRO implies a particular use for quality assurance or research on polymer concrete panels. To guarantee the structural integrity and functionality of these panels, it is essential to recognize their forms and flaws. Applying SRRO, forecasting models for polymer concrete panel form and fault identification may be optimized in a novel way. SRRO is a promising tool for enhancing the accuracy of shape and defect forecasting in this particular application because it adds randomness to the optimization process, which improves exploration, helps to escape local optima, and adapts well to the complexities present in real-world image data. The bio-inspired metaheuristic algorithm SRRO was proposed. This algorithm focuses on the social behavior of ravens and how individuals of the population communicate with one another to locate food. Ravens reside in groups of 200–10,000 throughout the non-breeding seasons of winter and fall. These groupings known as roosts or social sleep groups, develop on trees close to food sources. There is no clear explanation for social sleep. However, there are theories on these social groupings came to be: a) Roosting birds are less likely to be attacked by other animals. b) The roost may be thought of an information hub, a location where people from the group can exchange knowledge about where to get food. The SRRO algorithm was developed with inspiration from the social behavior of ravens and the way that individuals of the population communicate with one another to obtain food. The initial stage of this technique involves selecting a roost at random inside the field of space. Every N-member population is positioned in the search space at random. Each bird's location is given a fitness value, and the bird who finds the best answer is referred to the leader. A portion of the raven population follows the leader after leaving the roost. The area where the follower birds explore for food is a hyper sphere, which is the circle that surrounds the spot the leader identified earlier. The remaining population members fly in the direction of their preferred place and stay there to continue foraging. There are N phases in flying ravens. Equation (10) updates each bird's position in flight based on a selected step length.

$$x_{j,s} = x_{i,s-1} + c_{j,s} \tag{10}$$

Where  $x_{j,s}$  is the updated role of the jth raven  $x_{i,s-1}$  is the current standing of the jth raven, and  $c_{j,s}$  is an

arbitrary step size. The bird senses the condition of its halting location and surroundings within a radius.  $Q_{pept}$ . Provides samples  $M_{pept}$ . it enhanced the SRRO-EANN model, which improves polymer concrete panel shape and fault identification forecasting performance. By enhancing the quality control and inspection procedures and eventually lengthening the lifespan and dependability of buildings made of polymer concrete, this creative method has the potential to progress predictive technologies in the construction sector.

## 4. RESULT AND DISCUSSION

To construct an experimental procedure utilizing the scikit-learn (sklearn) module, Python 3, and the Keras neural network library. To compare our suggested model with the accuracy, precision, recall, MAE, and RMSE results that we saw with these existing approaches. The model provides both accuracy and Precision in the given hyper-parameter setting. In contrast, the systems that are able to attain maximum efficiency include VGG16 (Kim et al., (2022)), ResNet50 (Kim et al., (2022)), MobileNetV2 (Kim et al., (2022)), Adaboost (AB) (Rahman et al., (2021)), and Decision trees (DT) (Rahman et al., (2021)). When compared to existing models, the suggested SRRO-EANN produced positive results and offered an adequate performance.

### 4.1 Accuracy

The total number of accurate predictions multiplied through the entire sample represents accuracy, an outcome statistic that measures a classifier's overall effectiveness. It proves that categorization techniques can categorize data samples accurately. According to Equation (11), it is computed.

$$\text{Accuracy} = \frac{\text{True Positives (TP)} + \text{True Negatives (TN)}}{\text{True Positives (TP)} + \text{True Negatives (TN)} + \text{False Positives (FP)} + \text{False Negatives (FN)}} \tag{11}$$

Accuracy measure comparisons are shown in Figure 3 and Table 1. The SRRO-EANN value of the proposed approach is 99%, which is higher than the SRRO-EANN values of current methods like VGG16 (95.0%), ResNet50 (95.7%), and MobileNetV2 (97.6%). The proposed technique outperforms competing approaches when it comes to accurately categorizing artworks.

**Table 1.** Comparison of Accuracy.

Methods	Accuracy (%)
VGG16 (Kim et al., (2022))	95
ResNet50 (Kim et al., (2022))	95.7
MobileNetV2 (Kim et al., (2022))	97.6
SRRO-EANN [proposed]	99



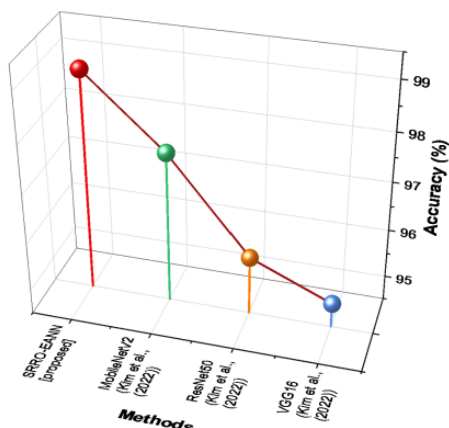


**Figure 3.** Accuracy comparisons between the suggested and current approaches

### 4.2 Precision

The ratio of accurately recognized occurrences to all instances with predicatively accurate information is known as Precision. One essential element of accuracy is Precision. To calculate the Precision, by Equation (12).

$$\text{Precision} = \frac{TP}{TP+FP} \quad (12)$$

The outcome of the suggested technique is shown in Table 2. Figure 4 displays the relative values of the various precision indicators. The proposed approach has an SRRO-EANN value of 97.9%, which is higher than the GA values of current methods like VGG16 (97.0%), ResNet50 (96.7%), and MobileNetV2 (93.6%). Compared to previous approaches, the SRRO-EANN proposed has better performance for polymer concrete panels.

**Table 2.** Comparison of Precision

Methods	Precision (%)
VGG16 (Kim et al., (2022))	97
ResNet50 (Kim et al., (2022))	96.7
MobileNetV2 (Kim et al., (2022))	93.6
SRRO-EANN (proposed)	97.9

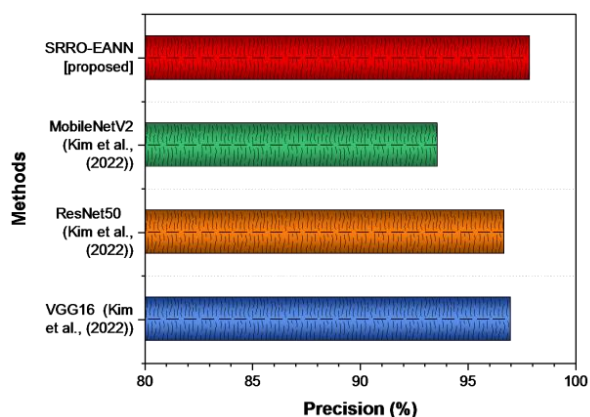


**Figure 4.** Precision comparisons between the suggested and current approaches

### 4.3 Sensitivity

The percentage of actual positive instances that are accurately classified as positive is known as sensitivity. It suggests that a different percentage of real positive cases mistakenly forecasted as negative. The definition of sensitivity is:

$$\text{Sensitivity} = \frac{TP}{TP+FN} \quad (13)$$

All the related sensitivity measurement comparison data exhibited sensitivity rates that were higher than normal VGG16, ResNet50, and MobileNetV2, with recognition of 95.6%, 94.7%, and 98.3%. Figure 5 and Table 3 represent the outcomes of recall. The proposed approach has an SRRO-EANN value of 98.86%.

**Table 3.** Comparison of sensitivity

Methods	Sensitivity (%)
VGG16 (Kim et al., (2022))	95.6
ResNet50 (Kim et al., (2022))	94.7
MobileNetV2 (Kim et al., (2022))	98.3
SRRO-EANN [proposed]	98.86

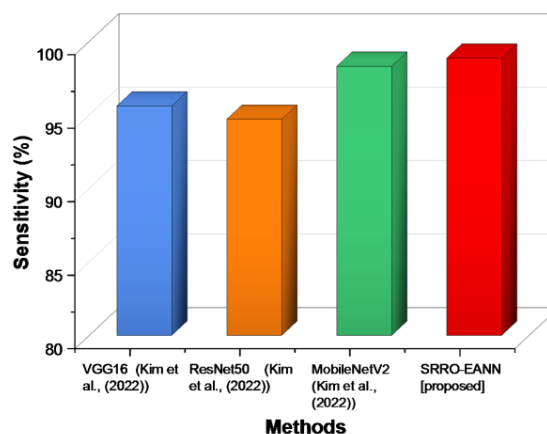


**Figure 5.** Sensitivity comparisons between the suggested and current approaches

### 4.4 Root Mean Square Error (RMSE)

The predictor's quality is assessed using the RMSE. By calculating the square root of the MSE, one may obtain the RMSE, or residual standard deviation of the samples.

$$RMSE = \sqrt{\frac{1}{m} \sum_{j=1}^m (z - z)^2} \quad (14)$$

SRRO-EANN achieved (0.042) comparatively with Adaboost (AB) (0.824) and Decision trees (DT) (0.089). It proves that the proposed process approach has lower rates than the existing methods.

### 4.5 Mean absolute error (MAE)

A statistic used to assess a prediction model's accuracy, especially in the context of regression analysis, is the MAE. It calculates the mean absolute difference between a dataset's actual values and its anticipated values.

$$MAE = \frac{1}{m} \sum_{j=1}^m |z - z| \quad (15)$$

SRRO-EANN achieved (0.014) comparatively with Adaboost (AB) (0.679), and Decision trees (DT) (0.029). It proves that the proposed process approach has lower rates than the existing method. The RMSE and MAE of the proposed system and the current system are both displayed in Table 4 and Figure 6.

**Table 4.** Comparison of RMSE and MAE

Methods	RMSE	MAE
Adaboost (Rahman et al., (2021))	0.824	0.679
Decision trees (Rahman et al., (2021))	0.089	0.029
SRRO-EANN (proposed)	0.042	0.014

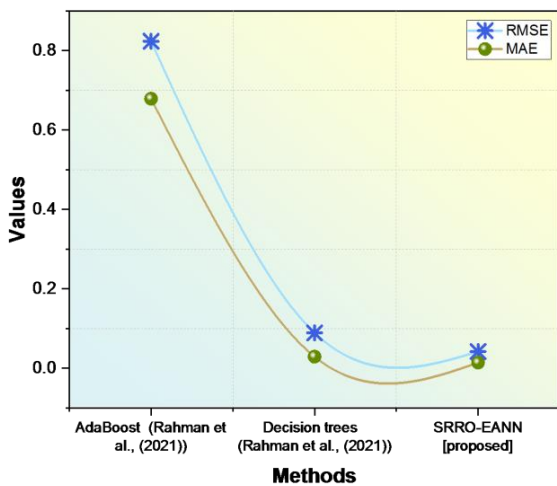


**Figure 6.** RMSE and MAE comparisons between the suggested and current approaches

### 4.6 F1-Score

An F1 score's accuracy and recall components are used to gauge a model performs in binary classification tasks. The accuracy of the model is computed as a single value that takes into account both measures. In this comparison, our proposed strategy obtains 96.3%, 95.7%, and 95.9%, whereas existing methods like VGG16, ResNet50, and MobileNetV2 reach the same results. It demonstrates that our suggested approach is better than the SRRO-EANN of 97%%. Figure 7 and Table 5 represent the outcomes of the F1-score.

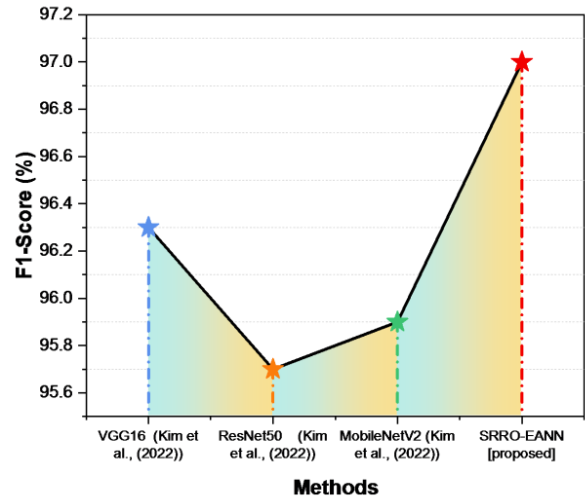


**Figure 7.** F1-score comparisons between the suggested and current approaches

$$F1 - score = \frac{(recall) \times (precision) \times 2}{recall + precision} \quad (16)$$

**Table 5.** Comparison of F1-score

Methods	F1-Score (%)
VGG16 (Kim et al., (2022))	96.3
ResNet50 (Kim et al., (2022))	95.7
MobileNetV2 (Kim et al., (2022))	95.9
SRRO-EANN (proposed)	97

### 4.7 DISCUSSION

Forecasting the identification of shapes and defects in polymer concrete panels can be challenging due to Adaboost sensitivity to noise, potential for over fitting, and limitations in handling complex relationships in the data. Despite its value, Adaboost is not a perfect algorithm for weak classifiers. Decision trees prefer to produce models that are too complicated and collect noise in the training data, which weakens the model. This sensitivity can lead to poor generalization performance and erroneous predictions, especially when dealing with the inherent variability in the emergence of faults or forms in polymer concrete. The receptive field of VGG16 is tiny and fixed. The model could have trouble capturing fine features or long-range relationships in huge pictures or complicated patterns in polymer concrete panels. ResNet50 functions on fixed-size input images and may have difficulties in grasping the relationships or global context between distant portions of an image. This constraint may make it more difficult for it to comprehend the context and general structure of polymer concrete panels, particularly when there are intricate forms or flaws present. SRRO-EANN can improve the solution space exploration and aid in the discovery of various neural network parameter settings. Finding the best configurations requires balancing exploration and exploitation, which is important for difficult tasks like defect discovery when

there may be a wide range of possible solutions. In this context, SRRO-EANN effectively addresses and surpasses the drawbacks inherent in existing methods.

## 5. CONCLUSION

To improved performance and durability, polymer concrete panels have become popular in the building industry. The development of precise and effective procedures for identifying forms and faults is necessary to provide the highest quality for these panels. By using sophisticated forecasting approaches to identify forms and defects in polymer concrete panels, this research makes a substantial contribution to the area. The growing use of polymer concrete panels in construction due to their superior

performance and durability calls for the creation of accurate and efficient procedures to guarantee the high caliber of these materials. In this study, we suggest using the SRRO-EANN to make encryption even more effective. As a consequence, we created an SRRO-EANN for classifying video data. Performance measures, including accuracy (99%), Precision (97.9%), F1-Score (97%), sensitivity (95%), RMSE (0.042), and MAE (0.014) are examined and compared with current technologies. Expand the future use of the SRRO-ANN model to encompass more categories of construction materials and manufacturing sectors. Evaluate the model's performance and adaptation in various environments to demonstrate its flexibility and effectiveness outside of polymer concrete panels.

## References:

- Amin, M. N., Iqbal, M., Jamal, A., Ullah, S., Khan, K., Abu-Arab, A. M., ... & Khan, S. (2022). Gep tree-based prediction model for interfacial bond strength of externally bonded frp laminates on grooves with concrete prism. *Polymers*,14(10), 2016.<https://doi.org/10.3390/polym14102016>.
- Asteris, P. G., Naseri, H., Hajihassani, M., Kharghani, M., &Chalioris, C. E. (2021). On the mechanical characteristics of fiber reinforced polymer concrete. *Adv. Concr. Constr*, 12, 271-282.<https://doi.org/10.12989/acc.2021.12.4.271>.
- Badra, N., Haggag, S. A., Deifalla, A., & Salem, N. M. (2022). Development of machine learning models for reliable prediction of the punching shear strength of FRP-reinforced concrete slabs without shear reinforcements. *Measurement*, 201, 111723.<https://doi.org/10.1016/j.measurement.2022.111723>.
- Cakiroglu, C., Islam, K., Bekdaş, G., Kim, S., &Geem, Z. W. (2022). Interpretable machine learning algorithms to predict the axial capacity of FRP-reinforced concrete columns. *Materials*, 15(8), 2742. <https://doi.org/10.3390/ma15082742>.
- Cheng, C., & Shen, Z. (2021). Semi real-time detection of subsurface consolidation defects during concrete curing stage. *Construction and Building Materials*, 270, 121489. <https://doi.org/10.1016/j.conbuildmat.2020.121489>.
- Dhiman, N. K., Sidhu, N., Agnihotri, S., Mukherjee, A., & Reddy, M. S. (2022). Role of nanomaterials in protecting building materials from degradation and deterioration. In *Biodegradation and Biodeterioration at the Nanoscale* (pp. 405-475). Elsevier.<https://doi.org/10.1016/B978-0-12-823970-4.00024-5>.
- Dolati, S. S. K., Malla, P., Ortiz, J. D., Mehrabi, A., &Nanni, A. (2023). Identifying NDT methods for damage detection in concrete elements reinforced or strengthened with FRP. *Engineering structures*, 287, 116155. <https://doi.org/10.1016/j.engstruct.2023.116155>.
- Dunaj, P., Berczyński, S., &Chodźko, M. (2020). Method of modeling steel-polymer concrete frames for machine tools. *Composite Structures*, 242, 112197. <https://doi.org/10.1016/j.compstruct.2020.112197>.
- Fodil, N., Chemrouk, M., & Ammar, A. (2021). Influence of steel reinforcement on ultrasonic pulse velocity as a non-destructive evaluation of high-performance concrete strength. *European Journal of Environmental and Civil Engineering*, 25(2), 281-301.<https://doi.org/10.1080/19648189.2018.1528890>.
- Gopal, K. N., Kumar, K. R. V., Jayaseelan, J., Suresh, G., Vezhavendhan, R., & Ganesamoorthy, R. (2023). Analyzing the Tribological Behavior of Titanium Dioxide (TiO<sub>2</sub>) Particulate Filled Jute Fiber Reinforced Interpenetrating Polymer Network (IPNs) Composite by using Taguchi Optimization Technique. *Tribology in Industry*, 45(1), 226–236. <https://doi.org/10.24874/ti.1448.02.23.04>
- Gupta, K., Hirani, H., & Muzakkir, S. M. (2023). Online Gear Wear Particle Detection and Categorization Using a Convolutional Neural Network Algorithm Integrated with Cascade Classifier. *Tribology in Industry*, 45(1), 212–225. <https://doi.org/10.24874/ti.1442.01.23.04>
- Jovicic, G., Milosevic, A., Sokac, M., Santosi, Z., Kocovic, V., Simunović, G., & Vukeli, D. (2023). The modelling of surface roughness after the turning of Inconel 601 by using artificial neural network. *Journal of Materials and Engineering*, 1(4), 179–188. <https://doi.org/10.61552/jme.2023.04.006>
- Kim, B., Choi, S. W., Hu, G., Lee, D. E., &Serfa Juan, R. O. (2022). An Automated Image-Based Multivariant Concrete Defect Recognition Using a Convolutional Neural Network with an Integrated Pooling Module. *Sensors*, 22(9), 3118. <https://doi.org/10.3390/s22093118>.



- Li, M., Pu, Y., Thomas, V. M., Yoo, C. G., Ozcan, S., Deng, Y., ... &Ragauskas, A. J. (2020). Recent advancements of plant-based natural fiber–reinforced composites and their applications. *Composites Part B: Engineering*, 200, 108254. <https://doi.org/10.1016/j.compositesb.2020.108254>.
- Liu, G. J., Bai, E. L., Xu, J. Y., Yang, N., & Wang, T. J. (2020). Dynamic compressive mechanical properties of carbon fiber-reinforced polymer concrete with different polymer-cement ratios at high strain rates. *Construction and Building Materials*, 261, 119995. <https://doi.org/10.1016/j.conbuildmat.2020.119995>.
- Mansourdehghan, S., Dolatshahi, K. M., &Asjodi, A. H. (2022). Data-driven damage assessment of reinforced concrete shear walls using visual features of damage. *Journal of Building Engineering*, 53, 104509. <https://doi.org/10.1016/j.job.2022.104509>.
- Nagajothi, S., &Elavenil, S. (2020). Experimental investigations on compressive, impact and prediction of stress-strain of fly ash-geopolymer and portland cement concrete. *Journal of Polymer Engineering*, 40(7),583-590.<https://doi.org/10.1515/polyeng-2020-0036>
- Philip, R. E., Andrushia, A. D., Nammalvar, A., Gurupatham, B. G. A., & Roy, K. (2023). A Comparative Study on Crack Detection in Concrete Walls Using Transfer Learning Techniques. *Journal of Composites Science*, 7(4),169.<https://doi.org/10.3390/jcs7040169>.
- Rahman, J., Ahmed, K. S., Khan, N. I., Islam, K., &Mangalathu, S. (2021). Data-driven shear strength prediction of steel fiber reinforced concrete beams using machine learning approach. *Engineering Structures*, 233, 111743. <https://doi.org/10.1016/j.engstruct.2020.111743>.
- Rautela, M., Senthilnath, J., Monaco, E., & Gopalakrishnan, S. (2022). Delamination prediction in composite panels using unsupervised-feature learning methods with wavelet-enhanced guided wave representations. *Composite Structures*, 291, 115579.<https://doi.org/10.1016/j.compstruct.2022.115579>.
- Rezaiee-Pajand, M., Karimipour, A., & Abad, J. M. N. (2021). Crack spacing prediction of fibre-reinforced concrete beams with lap-spliced bars by machine learning models. *Iranian Journal of Science and Technology, Transactions of Civil Engineering*, 45, 833-850.<https://doi.org/10.1007/s40996-020-00441-6>.
- Rezakhani, R., Scott, D. A., Bousikhane, F., Pathirage, M., Moser, R. D., Green, B. H., &Cusatis, G. (2021). Influence of steel fiber size, shape, and strength on the quasi-static properties of ultra-high performance concrete: Experimental investigation and numerical modeling. *Construction and Building Materials*, 296, 123532. <https://doi.org/10.1016/j.conbuildmat.2021.123532>.
- Yang, L., & Zhang, Y. (2023). Study on the preparation of high performance water reducer by nano-micron monomer in the durability of high performance concrete. *Ferroelectrics*, 608(1), 179-189.<https://doi.org/10.1080/00150193.2023.2198457>.

---

**Vinod Mansiram Kapse**

Noida Institute of Engineering & Technology,  
Greater Noida,  
Uttar Pradesh, India  
[director@niet.co.in](mailto:director@niet.co.in)  
ORCID 0000-0001-9123-9823

**Arun Kumar Marandi**

Arka Jain University,  
Jamshedpur,  
Jharkhand, India  
[dr.arun@arkajainuniversity.ac.in](mailto:dr.arun@arkajainuniversity.ac.in)  
ORCID 0000-0003-1507-7580

**Beemkumar Nagappan**

JAIN (Deemed-to-be University),  
Ramanagara District,  
Karnataka, India  
[n.beemkumar@jainuniversity.ac.in](mailto:n.beemkumar@jainuniversity.ac.in)  
ORCID 0000-0003-3868-0382

**Ankita Agarwal**

Maharishi University of Information Technology,  
Uttar Pradesh, India  
[agarwalankita.lko@gmail.com](mailto:agarwalankita.lko@gmail.com)  
ORCID 0000-0001-7539-8592

---

